Journal of Information Hiding and Multimedia Signal Processing ©2015 ISSN 2073-4212
Ubiquitous International Volume **6**, Number **6**, November **2015**

An Improving Analytically Model with High Accuracy for A Micro Manipulator

Yuan Ni, Zong-Quan Deng, Jun-Bao Li, Xiang Wu

Research Center of Aerospace Mechanism and Control
School of Mechatronics Engineering, Harbin Institute of Technology, China
ny1983119@hotmail.com, junbaolihit@gmail.com

Long Li

Shanghai Key Laboratory of Mechanical Automation and Robotics
SSchool of Mechatronic Engineering and Automation, Shanghai University, China
lil@shu.edu.cn

Received April, 2015; revised May, 2015

Abstract. *A proposed mathematical model is established for modal analysis of a micro manipulator. According to the geometric characteristics of the manipulator, the model is built by using finite element method with multipoint constraint equations, and the corresponding displacement coordinate matrix is obtained after that. Considering that the regular flexure hinge plays a key role, in this analysis process, the hinge is treated as a varied cross-section Euler-Bernoulli beam element and the finite element model is established by a new procedure which followed the element internal equilibrium principle consequently. The stiffness matrix, the mass matrix and the exact shape functions of the non-prismatic beam element can be obtained respectively. Furthermore, the influences of geometric parameters on the fundamental frequency can also be discussed.*
Keywords: Improving model; Micro manipulator; Natural frequency analysis.

1. **Introduction.** Micro manipulators are abundantly used in scientific instruments and precision engineering applications, such as adjustable posture institution of microwave antenna, scanning tunnel microscopy, bionic mechanism, micro-gripper, etc. These compliant mechanisms are manufactured integrally without assembling; and other characteristics include no friction, no backlash and low clearance make it easily to obtain high accuracy and reliability. A novel flexure-based 3-DOF mechanism which can achieve displacements in X,Y and ϕ in [1]. A proportion compliant mechanism is designed in [2] and proposed an analytical model based on the principle of virtual work and PRBM. A XY stage which is capable to scan over a relatively large range with high scanning speed is designed in [3]. A high-performance nano-positioning stage for high-bandwidth applications is presented in [4]. A parallel linear compliant mechanism is designed in [5] which is chiefly implemented by monolithically flexure hinges for two axes ultra-precision linear motion. 6-DOF flexure-based micro-manipulator is designed in [6] which is to be used as a fiber optics aligner is assembled by two parallel stages and these two stages have 3-DOF respectively. A large displacement precision XY positioning stage based on a novel designed cross strip flexure joint is presented in [7]. The flexure hinge, regarded as an essential factor for the micro manipulator, has been developed and investigated in the pertinent literature. Some works focused on the geometric configurations of the hinge

[8]-[13], it is indicated that closed-form compliance equations for diverse type of flexure hinges are very important. Accordingly, kinds of analytic approaches are utilized such as unit-load method, Castiglianos second theorem, elastic strain energy method, empirical equations established by the simulation analysis, the integration of linear differential equations, etc. Among those approaches used, finite element method drew much attention due to its some merits. The spatial stiffness matrix of the flexure hinge by using the finite element method is established in [14]. Another work regarded the single-axis circular flexure hinge as a three-node line element with 12-DOF in [15]. Flexure hinge here was taken as a varied cross-section in-plane Euler beam element with two-node in [16]. A similar work was followed in [17]. Second-order Hermite polynomial was utilized to establish shape functions of three-node non-prismatic beam element in order to enhance modal accuracy. In these researches, the flexure hinge was identified as a beam element with variable cross-section profile. Unfortunately, traditional displacement interpolation functions were not capable to describe unit displacement effectively [18], some researchers are focused on other methods. In [19], the exact shape functions were obtained by the analytical solutions of the beam governing differential equation, but this situation is only comfortable for the beams with simply varied cross section profile. A new method by using element-based equilibrium to obtain the exact displacement interpolation functions was presented in [20]. A similar work [21] dedicated to propose the strain interpolating functions rather than the shape functions of Euler and Timoshenko beam elements. The aim of this research is to present the modal analysis of a classic micro manipulator by using finite element procedure. The stiffness and mass matrices of the flexure hinge is established based on the thought of [20], which is treated as an in-plane two-node beam element with variable cross-section. The result of the mechanical modal analysis is compared to the FEA result to validate its accuracy.

2. **Free vibration analysis equations including multipoint restriction conditions.** The monolithic micro manipulator is composed of eight uniform-profile typical flexure hinges. When the manipulator is assembled into the practical application equipment combing with PZT, the dynamics analysis should be implemented. As a geometric unit, the flexure hinge is treated as the non-prismatic beam by using an efficient procedure, the stiffness and mass matrices will be discussed in the next section. Besides, eccentric distances exist between some nodes. This, in this paper, will adopt the multipoint constraint equations to simulate the excursions. Based on the finite element method, one of the most effective Energy principles, Hamilton principle, can be used to solve structural dynamics problem, one yield:

$$\delta \int_{t1}^{t2} L dt = 0 \tag{1}$$

where L is Lagrange functional and yields:

$$L = E_p - \Pi + \mathrm{W}_f \tag{2}$$

where E_p, Π and W_f represent the system kinetic energy, strain energy and external work respectively, and $E_p = \frac{1}{2} D_e^T M D_e, \prod = \frac{1}{2} D_e^T K D_e, \mathrm{W}_f = D_e^T F$.

In this case, considering the nodal eccentric distances, some compatibility equations should be added, it can be expressed by:

$$C D_e - Q = 0 \tag{3}$$

Combining the Eq.2 and Eq.3 and the correction functional L* can be expressed as:

$$L^* = \frac{1}{2}\dot{D}_e^T M \dot{D}_e - \frac{1}{2} D_e^T K D_e + D_e^T F - \lambda^T (C D_e - Q) \tag{4}$$

where λ is lagrangian multiplier.

Changing the sequences of the variation and integration, and by Hamilton principle one can obtain that:

$$\delta L^* = -\delta D_e^T M \ddot{D}_e - \delta D_e^T K D_e + \delta D_e^T F - \delta\lambda^T (C D_e - Q) - \lambda^T C \delta D_e = 0 \tag{5}$$

Considering that $\lambda^T C \delta D_e = \delta D_e^T C^T \lambda$, and Eq.5 can be rewritten as:

$$\delta D_e^T M \ddot{D}_e + \delta D_e^T K D_e - \delta D_e^T F + \delta\lambda^T Q + \delta D_e^T C^T \lambda = 0 \tag{6}$$

and

$$\begin{pmatrix} \delta D_e^T & \delta\lambda^T \end{pmatrix} \begin{bmatrix} M & 0 \\ 0 & 0 \end{bmatrix} \begin{pmatrix} \ddot{D}_e \\ \ddot{\lambda} \end{pmatrix} + \begin{pmatrix} \delta D_e^T & \delta\lambda^T \end{pmatrix} \begin{bmatrix} K & C^T \\ C & 0 \end{bmatrix} \begin{pmatrix} D_e \\ \lambda \end{pmatrix} = \begin{pmatrix} \delta D_e^T & \delta\lambda^T \end{pmatrix} \begin{pmatrix} F \\ Q \end{pmatrix} \tag{7}$$

considering that δD_e and $\delta\lambda$ are arbitrary and the system finite element equations with the additional constrained conditions can be obtained as

$$\begin{bmatrix} M & 0 \\ 0 & 0 \end{bmatrix} \begin{pmatrix} \ddot{D}_e \\ \ddot{\lambda} \end{pmatrix} + \begin{bmatrix} K & C^T \\ C & 0 \end{bmatrix} \begin{pmatrix} D_e \\ \lambda \end{pmatrix} = 0 \tag{8}$$

3. **Derivation of the system multipoint constraint equations and matrix C.** The traditional micro manipulator is symmetric, consequently, there are two groups of situations need to establish the constraint equations. The key to establish the constraint equations is to utilize the kinematic relationships of the nodal degrees of freedom. The constraint equations can be obtained as:

$$\begin{cases} d_{i1} = q_1 - l_y q_3 \\ d_{i2} = q_2 \\ d_{i3} = q_3 \\ d_{j1} = q_1 \\ d_{j2} = q_2 + l_x q_3 \\ d_{j3} = q_3 \end{cases} \tag{9}$$

eliminating the degrees freedom of the rigid body q_1, q_2 and q_3, we can obtain three equations as:

$$\begin{cases} d_{i1} + l_y d_{i3} - d_{j1} = 0 \\ d_{i2} + l_x d_{i3} - d_{j2} = 0 \\ d_{i3} - d_{j3} = 0 \end{cases} \tag{10}$$

Another group can be performed to obtain another group of constraint equations:

$$\begin{cases} d_{m1} - l_y d_{m3} - d_{n1} = 0 \\ d_{m2} + l_x d_{m3} - d_{n2} = 0 \\ d_{n3} - d_{m3} = 0 \end{cases} \tag{11}$$

4. **Derivation of the element matrices of the flexure hinge.**

4.1. **Element stiffness matrix.** The cross section height t, the area A and the moment of inertia I of the hinge can express by means of functions of the length of the hinge x in Eqs.12-14 respectively. It can be treated as a non-prismatic beam element with two nodes in plane in the element coordinate system, and each node has three degrees of freedom. Neither of boundary conditions applies on the beam element obviously, there are 3 DOFs that relate to the rigid body motion consequently. For the purpose of eliminating the rigid body motion, in the generalized element coordinate system, node 1 is restrained and the beam element has three independent deformations.

$$t(x) = 2r + t - 2\sqrt{r^2 - (r-x)^2} \tag{12}$$

$$A(x) = bt(x) = b(2r + t - 2\sqrt{r^2 - (r-x)^2}) \tag{13}$$

$$I(x) = \frac{bt(x)^3}{12} = \frac{b(2r + t - 2\sqrt{r^2 - (r-x)^2})^3}{12} \tag{14}$$

According to the beam theory, the displacement of an arbitrary node in the plane beam element can be expressed as follows:

$$u(x,y) = \left\{ \begin{array}{c} u_x(x,y) \\ u_y(x,y) \end{array} \right\} = \left\{ \begin{array}{c} u(x) - y\theta(x) \\ v(x) \end{array} \right\} \tag{15}$$

where $u(x), v(x)$ and $\theta(x)$ are the axial displacement, longitudinal displacement and angle displacement with respect to x, respectively.
The corresponding strain ε(x, y) can be derived from Eq. 16 as follows:

$$\varepsilon(x,y) = \left\{ \begin{array}{c} \varepsilon_{xx}(x,y) \\ \gamma_{xy}(x,y) \end{array} \right\} = \left\{ \begin{array}{c} \frac{\partial u_x(x,y)}{\partial x} = \frac{du(x)}{dx} - y\frac{d\theta(x)}{dx} \\ \frac{\partial u_x(x,y)}{\partial y} + \frac{\partial u_y(x,y)}{\partial x} = -\theta(x) + \frac{dv(x)}{dx} \end{array} \right\} \tag{16}$$

According to the Euler-Bernoulli beam theory, shear deformation does not take part in the strain vector, hence $\gamma_{xy}(x,y)$is equal to zero. Eq. 16 can be rewritten as:

$$\varepsilon(x,y) = \varepsilon_{xx}(x,y) = a\varepsilon_k \tag{17}$$

Where $a = (1-y)^T$ and $\varepsilon_k = (\frac{du(x)}{dx} \ \frac{d\theta(x)}{dx})^T$ The relationship between the internal force σ_k and the axial deformation ε_k is:

$$\sigma_K == \int_A a^T ca\varepsilon_K dA \tag{18}$$

where $\sigma_K = (N(x) \quad M(x))^T$

The tangent stiffness matrix of the cross section $K^s(x)$ is obtained by:

$$K^s(x) = \frac{\partial \sigma_K}{\partial \varepsilon_K} = \int_A a^T Ea dA \tag{19}$$

Meanwhile, the element flexibility matrix in element coordinate system is then derived by:

$$C^e = \int_0^1 b(x)^T K_s^{-1}(x) b(x) dx \tag{20}$$

where $b(x)$ is the transformation matrix to obtain internal section forces in the generalized element coordinate system:

$$\sigma_K = b(x)P \tag{21}$$

where P is the nodal forces $P = (F_x F_y F_z)^T$ and $b(x) = \begin{pmatrix} 1 & 0 & 0 \\ 0 & (2r-x) & 0 \end{pmatrix}$ The element stiffness K^e is then computed by Eq. 22 after the nodal forces transformation matrix T is obtained according Figs.4 (a) and (b).

$$K^e = TC^{e^{-1}}T^T \tag{22}$$

where $T = \begin{bmatrix} -1 & 0 & 0 & 1 & 0 & 0 \\ 0 & -1 & -l & 1 & 0 & 0 \\ 0 & 0 & -1 & 0 & 0 & 1 \end{bmatrix}^T$

4.2. **Element mass matrix and the shape functions.** According to the previous analysis, in the course of the derivation of the element stiffness matrix, there are no displacement interpolation functions. Hence, the primary aim is to describe internal displacement field by using the nodal displacements, then the mass matrix are established naturally.

In the element coordinate system, the axial displacement $u^e(x)$, longitudinal displacement $v^e(x)$ with respect to the arbitrary coordinate x can be expressed as:

$$u^e(x) = N_1(x)D_1^e + N_4(x)D_4^e \tag{23}$$

$$v^e(x) = N_2(x)D_2^e + N_3(x)D_3^e + N_5(x)D_5^e + N_6(x)D_6^e \tag{24}$$

where

$$N_1 = 1 - \frac{\int_0^x \frac{1}{EA(x_0)}dx_0}{\int_0^{2r} \frac{1}{EA(\xi)}d\xi}$$

$$N_2 = 1 - \frac{\int_0^{2r} \frac{1}{EI(\xi)}d\xi \int_0^x \frac{(x-x_0)(x_0-2r)}{EI(x_0)}dx + \int_0^{2r} \frac{(l-\xi)}{EI(\xi)}d\xi \int_0^x \frac{(x-x_0)}{EI(x_0)}dx_0}{\int_0^{2r} \frac{1}{EI(\xi)}d\xi \int_0^{2r} \frac{(\xi-l)^2}{EI(\xi)}d\xi - (\int_0^{2r} \frac{(l-\xi)}{EI(\xi)}d\xi)^2} - \frac{x}{2r}$$

$$N_3 = \frac{(-2r\int_0^{2r} \frac{1}{EI(\xi)}d\xi - \int_0^{2r} \frac{(l-\xi)}{EI(\xi)}d\xi) \int_0^x \frac{(x-x_0)(2r-x_0)}{EI(x_0)}dx - (2r\int_0^{2r} \frac{(l-\xi)}{EI(\xi)}d\xi + \int_0^{2r} \frac{(l-\xi)^2}{EI(\xi)}d\xi) \int_0^x \frac{(x-x_0)}{EI(x_0)}dx_0}{\int_0^{2r} \frac{1}{EI(\xi)}d\xi \int_0^{2r} \frac{(\xi-l)^2}{EI(\xi)}d\xi - (\int_0^{2r} \frac{(l-\xi)}{EI(\xi)}d\xi)^2}$$

$$N_4 = 1 - N_1 = \frac{\int_0^x \frac{1}{EA(x_0)}dx_0}{\int_0^{2r} \frac{1}{EA(\xi)}d\xi}$$

$$N_5 = \frac{\int_0^{2r} \frac{1}{EI(\xi)}d\xi \int_0^x \frac{(x-x_0)(x_0-2r)}{EI(x_0)}dx + \int_0^{2r} \frac{(l-\xi)}{EI(\xi)}d\xi \int_0^x \frac{(x-x_0)}{EI(x_0)}dx_0}{\int_0^{2r} \frac{1}{EI(\xi)}d\xi \int_0^{2r} \frac{(\xi-l)^2}{EI(\xi)}d\xi - (\int_0^{2r} \frac{(l-\xi)}{EI(\xi)}d\xi)^2} + \frac{x}{2r}$$

$$N_6 = \frac{\int_0^{2r} \frac{(l-\xi)}{EI(\xi)}d\xi \int_0^x \frac{(x-x_0)(2r-x_0)}{EI(x_0)}dx_0 + \int_0^{2r} \frac{(\xi-l)^2}{EI(\xi)}d\xi \int_0^x \frac{(x-x_0)}{EI(x_0)}dx_0}{\int_0^{2r} \frac{1}{EI(\xi)}d\xi \int_0^{2r} \frac{(\xi-l)^2}{EI(\xi)}d\xi - (\int_0^{2r} \frac{(l-\xi)}{EI(\xi)}d\xi)^2}$$

Then, the element mass matrix can be calculated by:

$$M^e = \int_0^{2r} \rho A(x) N^T(x) N(x) dx \tag{25}$$

where ρ is the material density, and $N(x) = \begin{bmatrix} N_1 & 0 & 0 & N_4 & 0 & 0 \\ 0 & N_2 & N_3 & 0 & N_5 & N_6 \end{bmatrix}$
Considering that the mass of rigid body in Fig.2 should be distributed to nodes, and the mass matrix of the flexure hinge can be rewritten as:

$$M^e = \int_0^{2r} \rho A(x) N^T(x) N(x) dx + N^T(x) \begin{bmatrix} \frac{1}{2}m_x & 0 \\ 0 & \frac{1}{2}m_y \end{bmatrix} \tag{26}$$

5. **Modal analysis with FEA and parameters influences analysis.** In this section, the analytical modal of the micro manipulator is validated by ANSYS modal analysis. The operational structural parameters are the same as [22]. As the same procedures in the previous static analysis, the mechanical amplifier 3D model is meshed by solid-186 element and the bottom of the amplifier is fixed. As shown in Fig.1, the first natural

frequency is 74.58Hz by utilizing the theoretical model, comparing with 69.73Hz which is obtained from the modal analysis, one finds that the result from the theoretical analysis model is close to that of ANSYS simulation. It is found that the use of the theoretical model is reliable, and it can be used to implement the optimal design.

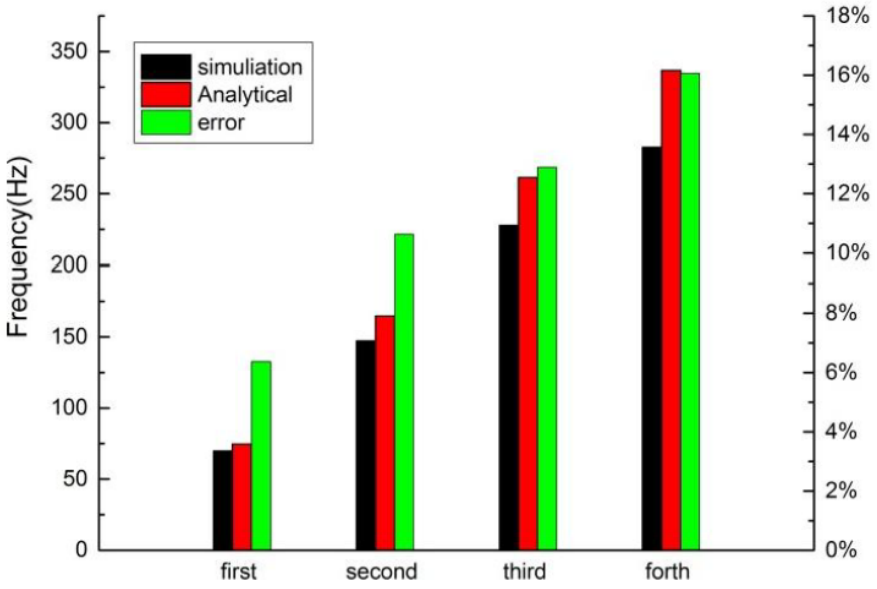

FIGURE 1. The first forth mode frequencies of the micro manipulator

A parametric study is carried on to investigate the influences of the key geometric parameters on the natural frequency of the mechanical amplifier.

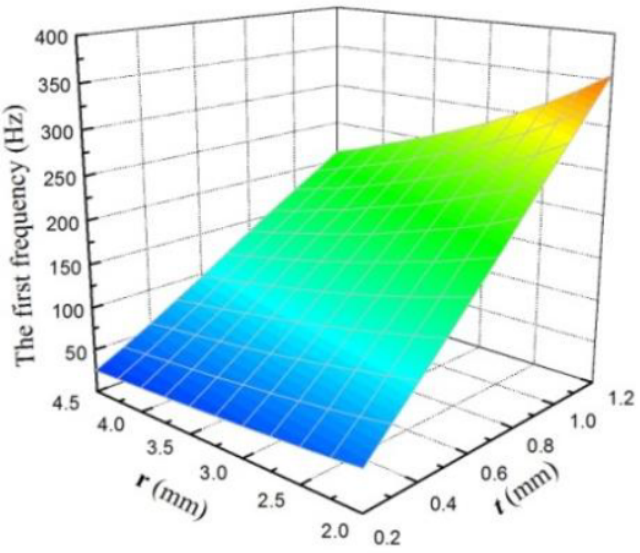

FIGURE 2. Influence of the ratio r and neck thickness t on the first frequency f

As shown in Fig.2, one can find that with the r is ascending; the first frequency is descending, which is opposite to the variation tendency with respect to the t. Fig.3 shows

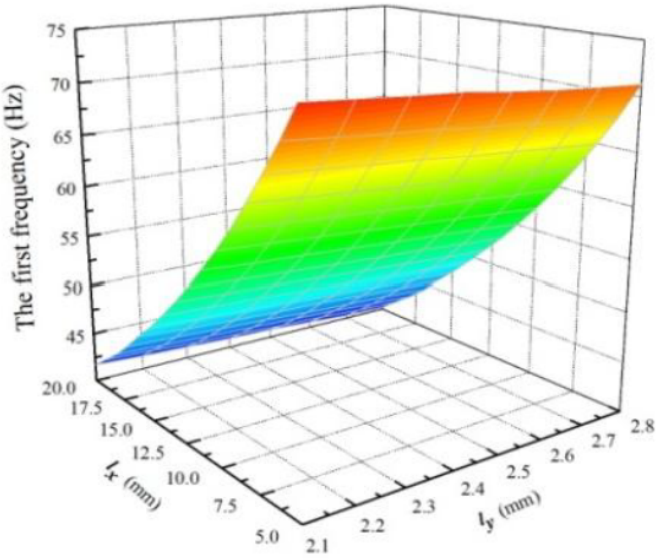

FIGURE 3. Influence of the l_x and l_y on the first frequency f

the variation tendencies of the first frequency with respect to the geometric parameters l_x and l_y. From Fig.3, one can find that with the parameters increase, both of l_x and l_y would lead the first frequency to decrease. The difference is the tendency with regard to the l_x is more sensitive. Comparing results from these two groups, one can find that t had a biggest impact on the first frequency, its value changes much considerable when t varies at the range of $0.2mm - 1.2mm$.

6. **Conclusions.** This research focuses on the issue of modal analysis of micro manipulator. Flexure hinge is regarded as the non-prismatic beam elements, and the system finite element equations with multipoint constraint equations are established consequently. After the model validation, the influences of the geometric parameters on the natural frequency of the mechanical amplifier are discussed. The results indicate that, with the increases of r, l_x and l_y, the natural frequency would decrease, and t has the biggest impact on the frequency.

REFERENCES

[1] U. Bhagat, B. Shirinzadeh, L. Clark, Design and analysis of a novel flexure-based 3-DOF mechanism, *J.Mechanism and Machine Theory*, vol. 74, pp. 173-187, 2014.

[2] Q. Meng, Y. Li, A novel analytical model for flexure-based proportion compliant mechanisms, *Proc. on IFAC symposium on mechatronic systems*, pp. 612-619, 2013.

[3] Y. Yuen, S. Sumeet, Design, Identification, and Control of a Flexure-Based XY Stage for Fast Nanoscale Positioning, *IEEE Trans. on nanotechnology*, vol. 8, pp.46-54, 2009.

[4] B. J. Kenton, K. K. Leang, Design, characterization, and control of a monolithic three-axis high-bandwidth nanopositioning stage, *Proc. on American Control Conference*, pp. 4949-4956, 2010.

[5] K. Choi, D. Kim, Monolithic parallel linear compliant mechanism for two axes ultraprecision linear motion, *J. Review of scientific instruments*, no. 77, 2006.

[6] D. Chao, G. Zong, R.Liu, Design of a 6-DOF compliant manipulator based on serial-parallel architecture, *Proc. of the 2005 IEEE/ASME International Conference on Advanced Intelligent Mechatronics*, pp. 765-770, 2005.

[7] Y. J. Choi, S.V. Sreenivasan, B.J. Choi, Kinematic design of large displacement precision XY positioning stage by using cross strip flexure joints and over-constrained mechanism, *J. Mechanism and Machine Theory,* vol. 43, pp. 724-737, 2008.

[8] G. Chen, J.Y. Jia, Z.W. Li, Study on hybrid flexure hinge, *Proceedings of Asia international symposium on mechatronics*, pp. 126-130, 2004.

[9] Q. Liu, H. Weng, L. Qiu, Compliances calculation and behavior analysis of the half right circular-elliptical hybrid flexure hinge, *J. Engineering Mechanics,* vol. 27, pp. 52-56, 2010.
[10] Y. Tian, B. Shirinzadeh, D. Zhang, Closed-form compliance equations of filleted V-shaped flexure hinges for compliant mechanism design, *J. Precision Engineering*, vol. 34, no. 3, pp. 408-418, 2010.
[11] Q. Li, C. Pan, X. J. Xu, Closed-form compliance equations for power-function-shaped flexure hinge based on unit-load method, *J. Precision Engineering*, vol. 37, no. 1, pp. 135-145, 2013.
[12] V. D. Lee, J. M. Gibert, J. C. Ziegert, Hybrid bi-directional flexure joint, *J. Precision Engineering*,vol. 38, no. 2, pp. 270-278, 2014.
[13] N. Lobontiu, M. Cullin, In-plane elastic response of two-segment circular-axis symmetric notch flexure hinges: The right circular design, *J. Precision Engineering*, vol. 37, no. 3, pp. 542-555, 2013.
[14] S. Zhang, E.D. Fasse, A Finite-Element-Based Method to Determine the Spatial Stiffness Properties of a Notch Hinge, *Journal of Mechanical Design*, vol. 123, no. 1, pp. 141-147, 2001.
[15] N. Lobontiu, E. Garcia, Circular-Hinge Line Element for Finite Element Analysis of Compliant Mechanisms, *Journal of Mechanical Design*, vol. 127, pp. 766-773, 2005.
[16] H. Wang, X. Zhang, Input coupling analysis and optimal design of a 3-DOF compliant micro-positioning stage, *Mechanism and Machine Theory*, vol.43, pp.400-410, 2008.
[17] X. Zhang, W. Hou, Dynamic analysis of the precision compliant mechanisms considering thermal effect, *Precision Engineering*, vol.34, no. 3, pp. 592-606, 2010.
[18] S. Li, X. Li, Y. B, Analysis of beam with variable cross-section by using direct element-based equilibrium framework, *Chinese Journal of computational mechanics*, vol. 26, no. 2, pp. 226-231, 2009.
[19] R. Filippo, Z. Gaetano, Deflections of beams with varying rectangular cross section, *Journal of engineering mechanics*, vol.118, no. 10, pp. 2128-2134, 1992.
[20] S. Li, J. Hu, C. Zhai, L. Xie, A unified method for modeling of axially and/or transversally functionally graded beams with variable cross-section profile, *Mechanics based design of structures and machines*, vol. 41, pp. 168-188, 2013.
[21] A. Shooshtari, R. Khajavi, An efficient procedure to find shape functions and stiffness matrics of nonprismatic Euler-Bernoulli and Timoshenko beam elements, *European Journal of Mechanics A/Solids*, vol. 29, pp. 826-836, 2010.
[22] Y. Ni, Z. Deng, X. Wu, Modeling and analysis of an over-constrained flexure-based compliant mechanism, *J. Measurement*, vol. 50, pp. 270-278, 2014.